Original Article

Pericarotid adipose tissue computed tomography attenuation distinguishes different stages of carotid atherosclerotic disease: a cross-sectional study

Xin Liu[1]^, Fang Wu[2], Xiuqin Jia[1], Huiyu Qiao[3], Yuehong Liu[1], Xiaoxu Yang[1], Yingying Li[1], Mengke Zhang[4], Qi Yang[1,5,6,7]^

[1]Department of Radiology, Beijing Chaoyang Hospital, Capital Medical University, Beijing, China; [2]Department of Radiology, Xuanwu Hospital, Capital Medical University, Beijing, China; [3]Center for Biomedical Imaging Research, Department of Biomedical Engineering, Tsinghua University School of Medicine, Beijing, China; [4]Department of Neurology, Xuanwu Hospital, Capital Medical University, Beijing, China; [5]Beijing Laboratory for Cardiovascular Precision Medicine, Beijing, China; [6]Key Laboratory of Medical Engineering for Cardiovascular Disease, Ministry of Education, Beijing, China; [7]Laboratory for Clinical Medicine, Capital Medical University, Beijing, China

Contributions: (I) Conception and design: X Liu, Q Yang; (II) Administrative support: Q Yang; (III) Provision of study materials or patients: X Liu, M Zhang; (IV) Collection and assembly of data: X Liu, F Wu; (V) Data analysis and interpretation: X Liu, Y Liu, Y Li; (VI) Manuscript writing: All authors; (VII) Final approval of manuscript: All authors.

Correspondence to: Qi Yang, MD, PhD. Department of Radiology, Beijing Chaoyang Hospital, Capital Medical University, No. 8 Gongti South Road, Beijing 100020, China; Beijing Laboratory for Cardiovascular Precision Medicine, Beijing, China; Key Laboratory of Medical Engineering for Cardiovascular Disease, Ministry of Education, Beijing, China; Laboratory for Clinical Medicine, Capital Medical University, Beijing, China. Email: yangyangqiqi@gmail.com.

Background: Carotid atherosclerotic plaque inflammation plays a critical role in guiding the prevention of secondary stroke. Increased perivascular adipose tissue attenuation observed on computed tomography angiography (CTA) may indicate local inflammation. Our objective was to investigate whether pericarotid adipose tissue (PCAT), as a local inflammation biomarker, could distinguish between different stages of carotid atherosclerotic disease plaques.

Methods: We prospectively enrolled 45 consecutive acute stroke patients with carotid artery stenosis from September 2019 to September 2021. We then matched them to non-stroke patients (n=67) and no carotid atherosclerotic disease controls (n=65) based on gender, age, and cardiovascular risk factors. We compared PCAT attenuation, carotid plaque features on CTA, clinical risk factors, and serum inflammatory factors across the different groups. To detect the association of PCAT attenuation with stage of carotid atherosclerotic disease, we used multivariable logistic regression analysis.

Results: Patients with acute stroke had a higher PCAT attenuation (–78.80±11.62 HU) than patients with non-stroke (–89.01±10.81 HU, P<0.001) and no carotid atherosclerotic disease controls (–95.24±10.81 HU, P<0.001). PCAT attenuation was significantly increased in non-stroke patients compared to non-stroke patients over no carotid atherosclerotic disease controls (P=0.004). The association between PCAT attenuation and the stage of carotid atherosclerotic disease was independent of age, gender, cardiovascular risk factors, and CTA plaque characteristics. No interaction was observed between clinical features and CTA plaque characteristics on PCAT attenuation.

Conclusions: PCAT attenuation, which is an imaging biomarker of local inflammation, independently distinguishes patients with different stages of carotid atherosclerotic disease. Quantitative evaluation of PCAT attenuation in carotid atherosclerotic disease is expected to guide targeted surgical treatment of carotid plaque.

^ ORCID: Xin Liu, 0000-0002-0205-1851; Qi Yang, 0000-0002-5773-0456.

Keywords: Carotid atherosclerotic disease; adipose tissue; computed tomography angiography (CTA)

Submitted Apr 05, 2023. Accepted for publication Sep 11, 2023. Published online Oct 24, 2023.
doi: 10.21037/qims-23-454
View this article at: https://dx.doi.org/10.21037/qims-23-454

Introduction

Carotid atherosclerotic disease is a significant contributor to ischemic stroke events. Thromboembolism resulting from the rupture of vulnerable carotid atherosclerotic plaques accounts for at least 15–30% of all ischemic stroke events (1,2). Consequently, there is a growing interest in developing a new imaging biomarker to improve the identification of vulnerable carotid plaques and alter management strategies for stroke.

It is important to note that inflammation plays a significant role in the rupture of vulnerable plaque (3). Studies conducted at the histological level have demonstrated that a substantial infiltration of inflammatory cells can be observed in atherosclerotic plaques that are classified as culprit lesions (4,5). The degree of inflammation is correlated with the incidence of ischemic stroke. Therefore, precise identification of local plaque inflammation is essential for targeted therapies that aim at preventing cardiovascular events, including ischemic stroke.

At present, there are few easily accessible methods for the early detection of local plaque inflammation. The metabolic activity of inflammatory cells within carotid atherosclerotic plaque can be visualized and measured using ^{18}F-fluorodeoxyglucose positron emission tomography (6,7). However, this technique is not commonly used in clinical practice due to poor spatial resolution, radiation exposure, and cost. Consequently, a conventional imaging method that can evaluate local plaque inflammation early is essential for risk stratification.

Several studies have indicated that increased perivascular fat density on computed tomography angiography (CTA) can indirectly reflect local plaque inflammation (8). Inflammatory mediators released from diseased vascular segments can cause perivascular adipose tissue inflammation and alter the phenotype of perivascular adipocytes, which may be the cause of inflammation (9). This phenomenon has been demonstrated in coronary arteries (10-12). Since carotid atherosclerosis shares characteristics and mechanisms with coronary atherosclerosis (13), researchers have proposed new ideas that use CTA attenuation to evaluate carotid atherosclerotic plaque inflammation. Konishi *et al.* established that perivascular adipose tissue inflammation was associated with cardiac events in coronary arteries (14). However, no studies have shown a causal relationship between carotid plaque inflammation as demonstrated by pericarotid adipose tissue (PCAT) attenuation and downstream ischemic stroke.

Investigating the capability of PCAT to distinguish the stage of carotid atherosclerotic disease could provide valuable insights into the connection between carotid plaque inflammation and ischemic stroke, potentially aiding in the secondary prevention of stroke and targeted treatment of carotid plaque. In this cross-sectional study, we evaluated the association of PCAT attenuation with stage of carotid atherosclerotic disease to shed light on the relationship between local carotid inflammation and ischemic stroke to some extent.

Methods

Patient population

The study was conducted in accordance with the Declaration of Helsinki (as revised in 2013). The study was approved by the Ethics Committee of Xuanwu Hospital, and informed consent was obtained from all patients or their legal guardians. We prospectively enrolled consecutive first acute stroke patients with carotid artery stenosis who were admitted to our stroke center from September 2019 to September 2021 in Group 1 (acute stroke group). Inclusion criteria were as follows: carotid sonography showed moderate to severe stenosis (≥50% measured as defined by NASCET criteria). Exclusion criteria were as follows: (I) history of allergy to iodine contrast media or renal dysfunction (estimated glomerular filtration rate assessed by creatinine clearance <60 mL/min/1.73 m^2). (II) Aortic artery and ipsilateral anterior circulation intracranial artery arteriosclerosis with ≥50% stenosis. (III) Evidence of non-atherosclerotic cerebrovascular diseases (e.g., vasculitis, Moyamoya disease, fibromuscular dysplasia). (IV) Echocardiography evidence of cardiogenic embolism. (V) History of transluminal intervention. During the same period, we matched the outpatients with carotid artery

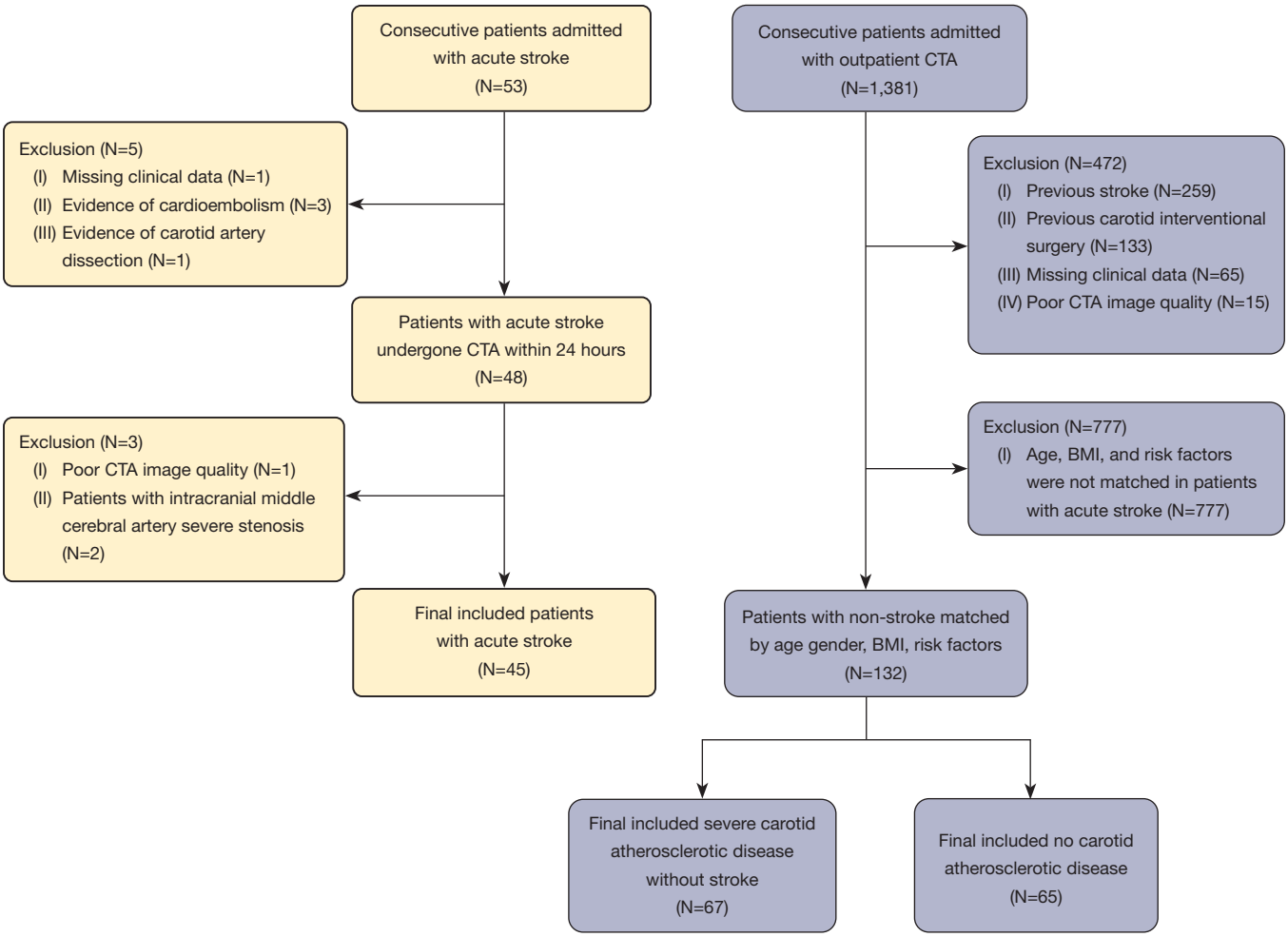

Figure 1 Flow chart. CTA, computed tomography angiography; BMI, body mass index.

stenosis severity ≥50% but without stroke (Group 2, non-stroke group), and with neither carotid artery stenosis nor stroke (Group 3, no carotid atherosclerotic disease group). We matched the three groups based on gender, age, and cardiovascular risk factors such as coronary heart disease, hypertension, diabetes, dyslipidemia, and smoking. Detailed medical records and laboratory data were recorded for all enrolled patients.

Please refer to *Figure 1* for a detailed description of the patient selection process. All patients underwent CTA and magnetic resonance imaging (MRI) examination within 24 hours after enrollment. CTA was used to evaluate carotid plaque features and PCAT, while MRI was employed to determine if the enrolled patients had experienced a recent stroke, which facilitated the process of patient grouping. We enrolled patients with acute stroke and carotid atherosclerotic plaques as culprit lesions which was determined by the neuroradiologist based on combined clinical and imaging information.

Imaging protocol

All patients underwent head and neck CTA using a 256-detector multi-detector CT scanner (Revolution CT, GE Healthcare, Milwaukee, USA). Data were acquired from the aortic arch to the vertex in a caudocranial direction. Imaging was performed before and after injection of contrast media. Images were obtained using prospective ECG-triggered axial scanning during one tube rotation and within one R-R interval. The tube voltage was 100 kVp. The tube current was adjusted based on attenuation and ranged from 350 to 650 mA. Enhanced

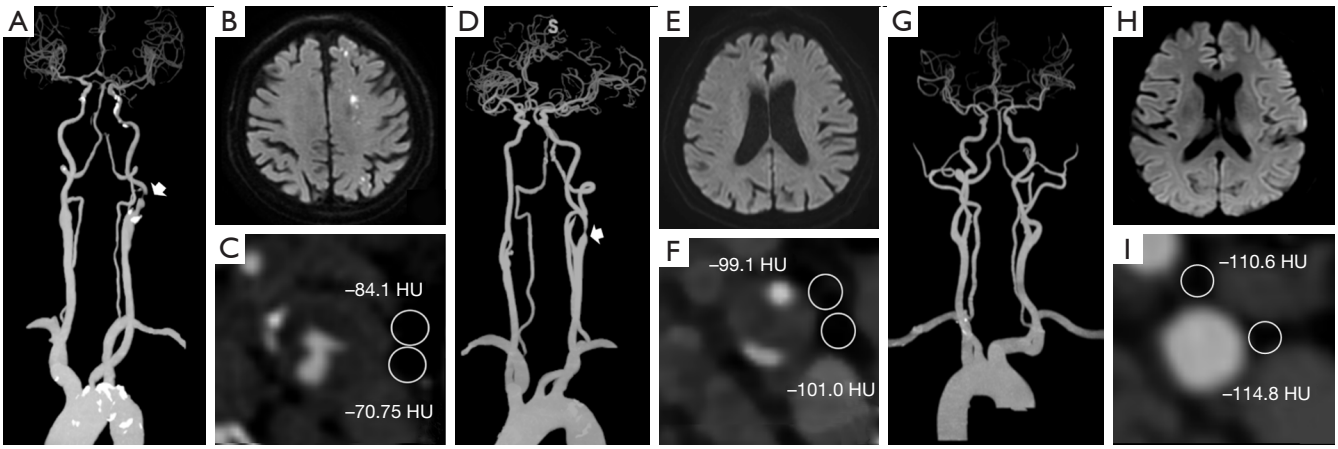

Figure 2 Measuring PCAT attenuation on CTA in three different groups. Patients with acute stroke (A-C), non-stroke (D-F), and no carotid atherosclerotic disease control (G-I). (A,D,G) MIP image shows severe stenosis of internal carotid artery (white arrows); (B,E,H) DWI image acute stroke, non-stroke, and no carotid atherosclerotic disease control; (C,F,I) axial CTA image shows different PCAT attenuation in three groups. HU, Housefield unit; PCAT, pericarotid adipose tissue; CTA, computed tomography angiography; MIP, maximum intensity projection; DWI, diffusion weighted imaging.

images were obtained by administering 60–80 mL of contrast medium (Ioversol, 320 Bayer Schering Pharma, Berlin, Germany). The scan started 8 seconds after the peak time of the ascending aorta. CT scan parameters were as follows: slice thickness of 0.625 mm, matrix size of 512×512, and a field of view of 14–19 cm. The original images had a slice thickness and spacing of 0.625 mm. Reconstructed images were obtained using the post-processing workstation (AW4.7, GE Healthcare). These images, including maximum intensity projection, multiplanar reformation, curved planar reformation, and volume rendering, were used to evaluate vascular characteristics.

Routine brain MRI was performed with a 3-tesla MRI scanner (Magnetom Verio, Skyra, Prisma, Siemens, Erlangen, Germany) with a 32-channel integrated head coil.

Imaging analysis

CTA image analysis

All CTA images were analyzed using VascuCAP software (Elucid Bioimaging, Wenham, MA, USA) (12) and assessed with viewing window settings of 850 HU/300 HU to evaluate CTA characteristics.

Qualitative features analysis

Qualitative features included plaque enhancement and plaque ulceration. Plaque ulceration was defined as a projection of contrast material at least 2 mm deep into the plaque in any single plane (15). Plaque enhancement was defined as the CT value of plaque increasing after administration of contrast (16).

Quantitative features analysis

Quantitative features included luminal stenosis, max dilation, soft plaque thickness, PCAT attenuation, and volumes of plaque components. Soft plaque thickness was defined as the maximum thickness of the noncalcified plaque component on CTA axial sections (17).

We placed the circular regions of interest (ROIs; 2.5 mm^2) in the adipose tissue near the two carotid arteries included in the final analysis. In Groups 1 and 2, we placed the ROIs within the adipose tissue adjacent to the symptomatic side or the narrowest carotid artery side, respectively. We positioned the other two ROIs at the same level near the contralateral carotid artery. In Groups 3, the ROIs were respectively placed in the adipose tissue surrounding the bifurcation of the bilateral carotid arteries, as this is a common site for plaque development. Carefully excluding the lumen, calcifications, and other soft tissue structures, we placed the ROIs at least 1 mm from the outer edge of the carotid wall. *Figure 2* shows examples of measuring PCAT attenuation on CTA from each of the three groups. The degree of luminal stenosis was also automatically determined by the software. The mean HU and standard deviation of the two ROIs were included in the final analysis.

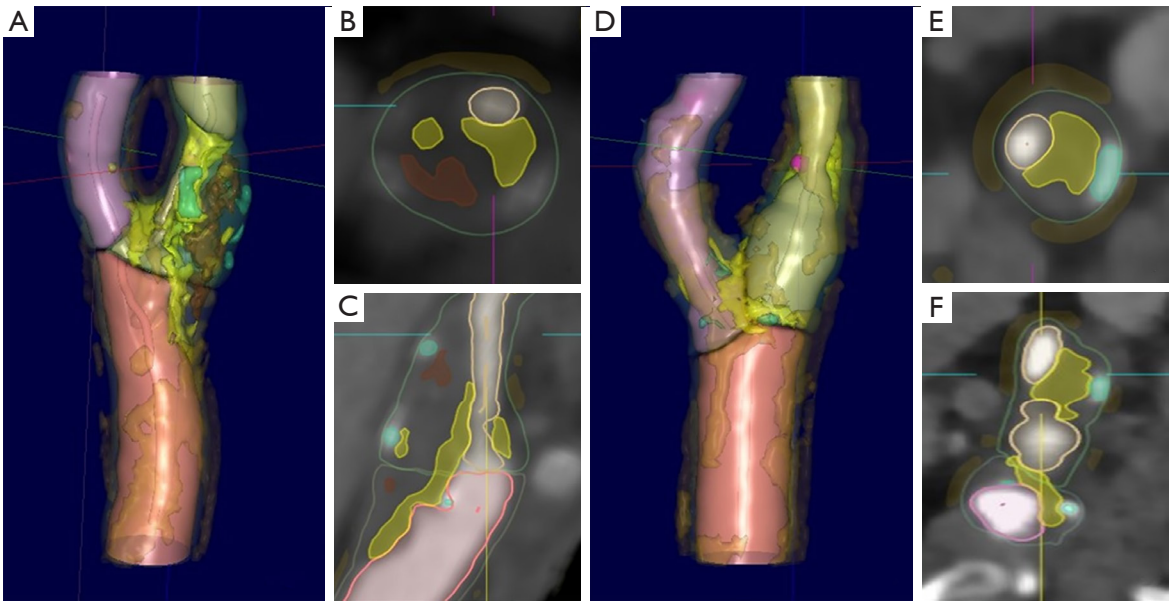

Figure 3 Example of semiautomatic segmentation with VascuCAP of the carotid artery plaque of two subjects. In acute stroke patient, (A-C) significant IPH components. In non-stroke patient, (D-F) lipid and calcium were the dominating plaque components. Red means IPH; Yellow means lipid; Green means calcium; Brown means PCAT; Other parts of the plaque component are mixed. IPH, intraplaque hemorrhage; PCAT, pericarotid adipose tissue.

The volumes of various plaque components were assessed using VascuCAP, a semiautomatic software (*Figure 3*) (12). We manually delineated lumen and wall of carotid plaque segments. Software segmentation of plaque components was based on the different CT value ranges for each element. Thresholds of each specific tissue were as follows (18): calcified (≥130 HU), mixed (≥60 and <130 HU), lipid (≥25 and <60 HU), and intraplaque hemorrhage (IPH) (<25 HU). The software automatically output percentage luminal stenosis and max dilation.

Statistical analysis

The Shapiro-Wilk test was used to check for normality. Descriptive statistics were used to report continuous variables as mean and standard deviation for normally distributed variables, and median and interquartile range for non-normally distributed variables. Categorical variables were reported as percentages. One-way ANOVA or Kruskal-Wallis testing with Bonferroni correction for post-hoc analysis was used to compare the three groups. The Chi-squared test was used for categorical variables. Multivariate logistic regression models were used to determine the contribution of PCAT attenuation to each stage of carotid atherosclerotic disease, adjusting for plaque characteristics or cardiovascular risk factors. Variables with a P value of ≤0.1 or recognized risk factors from univariate analysis were entered into the multivariate analysis model. Stepwise multifactor logistic regression analysis was performed to determine independent predictors of stroke or stable carotid atherosclerotic disease. Statistical significance was set at P value <0.05. The intraobserver and interobserver consistency of qualitative CTA characteristics were evaluated using Cohen's κ coefficient, and the consistency of quantitative CTA characteristics was evaluated using intraclass correlation coefficient. SPSS 25.0 (SPSS Inc., Chicago, IL, USA) and GraphPad Prism 7.0 for Windows (San Diego, CA, USA) were used for all statistical analyses.

Results

Demographic and clinical characteristics

The study included a total of 177 participants, with 45 acute stroke patients in Group 1, 67 non-stroke patients in Group 2, and 65 no carotid atherosclerotic disease controls in Group 3. *Table 1* presents the clinical characteristics of the

Table 1 Clinical laboratory characteristics of the study population

Variables	Group 1 (n=45)	Group 2 (n=67)	Group 3 (n=65)	P value		
				1 *vs.* 2	1 *vs.* 3	2 *vs.* 3
Clinical characteristics						
Age (years)	67.09±8.2	67.60±8.4	64.85±6.8	0.939	0.303	0.110
Male	42 (93.3)	56 (83.6)	54 (83.1)	0.126	0.113	0.938
BMI (kg/m^2)	24.6±3.4	24.6±3.2	25.7±3.9	0.957	0.748	0.718
Coronary heart disease	10 (22.2)	19 (28.4)	16 (24.6)	0.467	0.771	0.626
Hypertension	34 (75.6)	48 (71.6)	47 (72.3)	0.647	0.704	0.180
Diabetes	19 (42.2)	28 (41.8)	23 (35.4)	0.964	0.468	0.450
Dyslipidaemia	16 (35.6)	19 (28.4)	15 (23.1)	0.420	0.153	0.488
Smoking	24 (53.3)	32 (47.8)	33 (50.8)	0.563	0.791	0.730
Lipids (mmol/L)						
Triglyceride	1.27 (0.39–3.39)	1.05 (0.29–3.26)	1.04 (0.54–3.23)	1.138	0.888	0.326
Total cholesterol	3.77 (2.08–5.30)	3.55 (2.05–6.09)	3.69 (2.09–5.56)	0.357	0.883	0.583
HDL cholesterol	1.05 (0.83–1.71)	1.03 (0.69–1.68)	0.98 (0.59–2.22)	0.973	0.152	0.051
LDL cholesterol	2.19 (0.97–3.73)	2.03 (0.75–4.13)	2.11 (1.08–3.82)	0.139	0.140	0.126
Homocysteine	18.82 (7.70–95.10)	15.95 (5.30–34.40)	13.06 (1.90–19.90)	0.182	**0.002**	0.122
Inflammatory marks (mmol/L)						
High-sensitive C-reaction protein	1.38 (0.58–3.61)	0.92 (0.41–1.28)	0.88 (0.48–1.04)	**0.012**	**<0.001**	0.089

Values are expressed as n (%), mean ± standard deviations, or median (interquartile range, 25th–75th). Group 1 included patients with acute stroke due to carotid atherosclerosis disease; Group 2 included patients with carotid atherosclerosis disease and no stroke; Group 3 included patients with neither carotid atherosclerosis disease nor stroke. Bold face P values indicate statistical significance. BMI, body mass index; HU, Hounsfield units; LDL, low-density lipoprotein; HDL, high-density lipoprotein.

participants in the three groups. The groups were matched for gender, age, and cardiovascular risk factors such as coronary heart disease, hypertension, diabetes, dyslipidemia, and smoking. Regarding blood lipid laboratory tests, homocysteine levels were significantly higher in Group 1 compared to Group 3 (18.82 *vs.* 13.06 mmol/L, P=0.002). High-sensitive C reaction protein (Hs-CRP) levels were significantly higher in Group 1 compared to the other two groups (1.38 *vs.* 0.92 and 0.88 mmol/L, P=0.012 and <0.001, respectively).

PCAT attenuation among three groups

We compared the bilateral PCAT attenuation in the three different groups. In Group 1, the PCAT attenuation on the symptomatic side was significantly higher than that on the non-symptomatic side (–78.80±11.62 *vs.* –85.96±11.31 HU, P<0.001). In Group 2, the PCAT attenuation on the carotid severe stenosis side was significantly higher than that on the non-stenosis side (–89.01±10.81 *vs.* –97.66±7.12 HU, P<0.001). In Group 3, there was no significant difference in PCAT between right and left sides (–95.24±10.81 *vs.* –96.03±7.27 HU, P=0.183) (Figure S1). We conducted inter-group comparisons among the symptomatic side in Group 1, the stenosis side in Group 2, and either side of Group 3. *Table 2* presents the PCAT attenuation in the three groups. The results showed that PCAT attenuation was significantly higher in acute stroke patients (–78.80±11.62 HU) compared to non-stroke patients (–89.01±10.81 HU, P<0.001) and no carotid atherosclerotic disease controls (–95.24±10.81 HU, P<0.001) (*Figure 4*).

Other characteristics on CTA between the groups

In *Table 2*, carotid plaque characteristics were compared between Groups 1 and 2 since Group 3 (no carotid

Table 2 Plaque characteristics on CTA of the three groups

Variables	Group 1 (n=45)	Group 2 (n=67)	Group 3 (n=65)	P value
Percentage luminal stenosis (%)	87.18±12.92	84.84±14.90		0.304
Max dilation (%)	16.00 (4.00–48.00)	19.00 (7.00–28.00)		0.794
Plaque characteristics				
Soft plaque thickness, cm	3.74±1.21	3.50±1.45		0.348
Plaque enhancement	23 (51.1)	21 (31.3)		**0.036**
Plaque ulceration	19 (42.2)	22 (32.8)		0.312
Plaque component volume (mm^3)				
Calcium	105.86 (63.84–1,622.41)	88.47 (44.28–126.20)		**0.045**
Lipid	244.51 (211.68–431.77)	285.97 (208.68–409.70)		0.326
Mixed	664.54 (498.47–813.44)	586.63 (452.56–824.22)		0.295
IPH	8.11 (1.56–21.27)	2.98 (0.00–12.19)		**0.008**
PCAT attenuation (HU)				(Group 1 *vs.* 2, 1 *vs.* 3, 2 *vs.* 3)
Mean	−78.80±11.62	−89.01±10.81	−95.24±10.81	**<0.001, <0.001, 0.004**
Min	−97.62±12.69	−104.60±14.00	−110.65±14.83	**0.028, <0.001, 0.037**
Max	−53.49±12.43	−66.49±11.90	−72.46±12.97	**<0.001, <0.001, 0.018**
SD	12.68 (8.86–16.41)	14.40 (11.38–16.53)	11.93 (8.84–17.33)	0.209, 0.669, 0.625

Values are expressed as n (%), mean ± standard deviations, or median (interquartile range, 25th–75th). Group 1 included patients with acute stroke due to carotid atherosclerosis disease; Group 2 included patients with carotid atherosclerosis disease and no stroke; Group 3 included patients with neither carotid atherosclerosis disease nor stroke. Bold face P values indicate statistical significance. CTA, computed tomography angiography; IPH, intraplaque hemorrhage; PCAT attenuation, pericarotid adipose tissue attenuation; HU, hounsfield unit; SD, standard deviation.

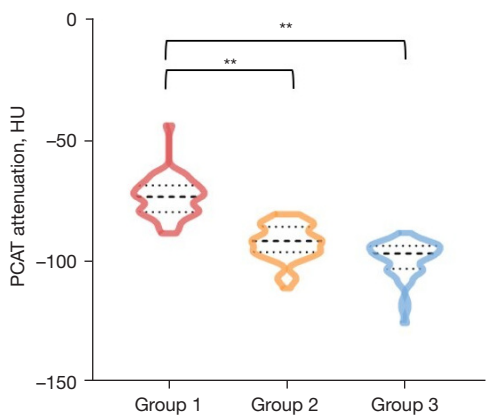

Figure 4 Comparison of PCAT attenuation among the three different groups. Group 1 included patients with acute stroke due to carotid atherosclerosis disease; Group 2 included patients with carotid atherosclerosis disease and no stroke; Group 3 included patients with neither carotid atherosclerosis disease nor stroke. **, P<0.001. PCAT, pericarotid adipose tissue.

atherosclerotic disease control group) did not have carotid artery stenosis. The percent of luminal stenosis and max dilation did not significantly differ between the two groups. Patients with acute stroke had a significantly greater IPH volume (8.11 *vs.* 2.98 mm^3, P=0.008) and calcium volume (105.86 *vs.* 88.47 mm^3, P=0.045) compared with non-stroke patients. Plaque enhancement on CTA was more frequent in the acute stroke group than in the non-stroke group (51.1% *vs.* 31.3%, P=0.036). The acute stroke group had a larger soft plaque thickness (3.74 *vs.* 3.50 cm, P=0.348) and a higher frequency of plaque ulceration (42.2% *vs.* 32.8%, P=0.312), although the differences were not statistically significant.

Multivariate analysis

To investigate the potential association between PCAT attenuation and stroke, we conducted multivariate logistic

Table 3 Multivariable logistic regression: association of PCAT attenuation with three groups

Variables	Univariate logistic regression			Multivariate logistic regression		
	Odd ratio	95% CI	P value	Odd ratio	95% CI	P value
Model 1 (Group1 *vs.* 2)						
Percentage luminal stenosis	1.012	0.984–1.042	0.391			
Max dilation	1.007	0.999–1.016	0.090			
Soft plaque thickness	1.144	0.865–1.514	0.346			
Plaque enhancement	2.290	1.050–4.995	0.037			
Plaque ulceration	1.495	0.685–3.264	0.313			
Calcium	1.006	1.000–1.012	0.046	1.021	1.003–1.040	**0.024**
Lipid	0.999	0.997–1.001	0.469			
Mixed	1.000	0.999–1.001	0.829			
IPH	1.029	1.003–1.057	0.032			
PCAT attenuation	1.579	0.469–4.490	<0.001	1.709	1.293–2.258	**<0.001**
Hs-CRP	1.485	1.141–1.933	0.003			
Model 2 (Group 2 *vs.* 3)						
Age (years)	1.063	1.015–1.112	0.009	1.076	1.022–1.220	**0.006**
Male	1.037	0.415–2.591	0.938			
Coronary heart disease	1.212	0.558–2.631	0.626			
Hypertension	0.968	0.453–2.069	0.932			
Diabetes	1.311	0.649–2.648	0.450			
Dyslipidaemia	1.748	0.769–3.975	0.183			
Smoking	0.887	0.448–1.755	0.730			
PCAT attenuation	1.144	1.075–1.217	<0.001	1.165	1.088–1.248	**<0.001**
Hs-CRP	1.550	0.965–2.491	0.070			

Model 1 adjusted for plaque features, PCAT attenuation and associated with carotid atherosclerosis disease. Model 2 adjusted for clinical indicators and PCAT attenuation associated with carotid atherosclerosis disease. Group 1 included patients with acute stroke due to carotid atherosclerosis disease; Group 2 included patients with carotid atherosclerosis disease and no stroke; Group 3 included patients with neither carotid atherosclerosis disease nor stroke. Bold face P values indicate statistical significance. IPH, intraplaque hemorrhage; PCAT attenuation, pericarotid adipose tissue attenuation; Hs-CRP, high-sensitive C reaction protein; CI, confidence interval.

regression analysis on Groups 1 and 2 by adjusting PCAT attenuation and other carotid plaque features. The analysis was adjusted for factors that had a P value <0.1 in the univariate analysis, including max dilation, plaque enhancement, calcium volume, IPH volume, PCAT attenuation, and Hs-CRP. In the multivariate analysis, calcium volume and PCAT attenuation remained significant (P<0.05), with odds ratios of 1.021 (95% CI, 1.003–1.040) and 1.709 (95% CI, 1.293–2.258), respectively (*Table 3*, Model 1).

To investigate the potential association between PCAT attenuation and stable carotid atherosclerotic disease, we conducted multivariate logistic regression analysis on Group 2 and Group 3 by adjusting PCAT attenuation and other clinical risk factors. The analysis was adjusted for age, PCAT attenuation, and Hs-CRP, which had a P value <0.1 in the univariate analysis. In the multivariate analysis, age and PCAT attenuation remained significant (P<0.05), with odds ratios of 1.076 (95% CI, 1.022–1.220) and 1.165 (95% CI, 1.088–1.248), respectively (*Table 3*, Model 2).

Interobserver agreement on CTA characteristics analysis

CTA imaging was evaluated by two neuroradiologists with five and ten years of experience. They were blinded to patient clinical data, and they did not know each other. Inter-reader correlation coefficients (ICC) for measurements of PCAT attenuation, soft plaque thickness, percentage luminal stenosis and max dilation were 0.82, 0.84, 0.87 and 0.88, respectively. The ICC values of volumes of plaque components, including calcium, lipid, mixed, and IPH volumes, were 0.92, 0.85, 0.89 and 0.82, respectively. For the inter-reader agreement in the identification of the presence of plaque enhancement and plaque ulceration, the K values were 0.90 and 0.86, respectively. The results indicated excellent interobserver reliability.

Discussion

In this cross-sectional study, we discovered that the PCAT attenuation, a novel biomarker of carotid inflammation, increases from stable carotid atherosclerotic disease to stroke. Multivariate analysis revealed that PCAT attenuation is independently associated with stable carotid atherosclerotic disease and the incidence of acute ischemic stroke. Thus, it is reasonable to assume that PCAT attenuation may aid in investigating the causal link between PCAT attenuation and acute stroke to some degree. These findings may offer fresh insights into early targeted secondary prevention in ischemic stroke and therapeutic interventions.

We discovered that PCAT attenuation was higher in the acute stroke group compared to the non-stroke group, independent of other plaque characteristics observed on CTA. This finding is consistent with a previous study by Baradaran *et al.*, who found that increased CT attenuation in the perivascular adipose tissue surrounding internal carotid artery (ICA) was associated with ipsilateral stroke or transient ischemic attack (19). This phenomenon may be linked to inflammation of the carotid plaque, which is a well-known response to local inflammatory processes. The CTA can detect the gradient of adipocyte size, which is expressed as an increase in CT attenuation, and can reflect the aggregation of inflammation. Inflammatory mediators such as TNF-α and IL-6 released by the diseased vascular wall inhibit adipogenesis in perivascular adipose tissue (20), causing a gradient of adipocyte size around the arterial wall. In fact, Oikonomou *et al.* reported that the increase of CT attenuation in pericoronary adipose tissue was significantly related to acute coronary syndrome (21). However, it is not clear whether increased PCAT attenuation precedes plaque rupture or not.

To explore whether PCAT was associated with stable carotid atherosclerotic disease, we included a no carotid atherosclerotic disease control group with no carotid plaque. Elevated PCAT was associated with the presence of carotid plaque when compared to the absence of carotid plaque. To our knowledge, our study is the first to stage carotid atherosclerotic disease (no carotid atherosclerotic disease control, non-stroke, acute stroke) in relation to PCAT attenuation. We further demonstrated that local inflammation of carotid plaque persists with plaque progression and that this inflammation can be detected on CTA.

Our findings are consistent with recent studies suggesting that high perivascular adipose tissue attenuation indicates an increased risk of cardiovascular events (10,19,22). Lin *et al.* (10) reported that pericoronary adipose tissue CT attenuation was an imaging biomarker of coronary inflammation, distinguishing different stages of coronary artery disease. Our study supports this finding, suggesting that perivascular adipose tissue CT attenuation varies with different stages of cardiovascular events. Baradaran *et al.* (19) also reported a greater mean pericarotid fat density (PFD) in symptomatic patients compared to asymptomatic patients. Zhang *et al.* (22) found that an increase in PFD was related to the risk of cerebrovascular symptoms. However, the study by Zhang *et al.* included only a limited number of other plaque vulnerability features. In our research, we bridged this gap by incorporating as many features of vulnerable plaques as possible using new semiautomatic software. It was essential to analyze the impact of multiple confounding factors on the risk of ischemic stroke.

We discovered that the calcification component of carotid plaque was greater in the acute stroke group than in the non-stroke group, and this association with stroke occurrence was independent of other plaque characteristics. These findings contradict previous research, which suggested that the calcification component was more stable. The reason for this discrepancy may be related to the overall plaque burden. Furthermore, a study by Zhang *et al.* (23) found that spotty calcification was significantly linked to the occurrence of non-lacunar ischemic stroke, which may also explain the significant correlation between the load of highly calcified plaques and the occurrence of stroke. However, as this study did not primarily investigate

the relationship between calcification and stroke, the correlation between calcification pattern and stroke was not explored.

In our study, multivariate regression analysis did not find a statistically significant difference in the Hs-CRP levels between the acute stroke group and the other two groups, despite the higher levels observed in the acute stroke group. Hs-CRP is a plasma biomarker that reflects the overall level of inflammation in the body (24). While numerous studies have shown that high levels of Hs-CRP are associated with an increased risk of cardiovascular events, plasma biomarkers do not provide information on atherosclerosis or local inflammation surrounding carotid atherosclerotic plaques (25,26). Targeted therapies for ischemic stroke must accurately detect local inflammation in carotid atherosclerotic plaques. A previous study suggested that one of the common features of vulnerable plaques is the abundance of inflammatory cells (27). However, assessing inflammation through routine clinical imaging is challenging.

Our study found that the acute stroke group had more plaque enhancement and a larger volume of IPH than the other two groups. Bentzon *et al.* reported that high levels of inflammatory cells in the adventitia can lead to local hypoxia and the formation of immature microvessels (28), which are prone to rupture and cause IPH (29). Plaque enhancement and IPH are both associated with an increased risk of plaque rupture and cerebrovascular symptoms (29,30). However, our multivariate analysis did not reveal significant differences in plaque enhancement and IPH volume among the groups, possibly due to the unclear relationship between these factors and PCAT. Saba *et al.* showed a positive association between PCAT attenuation and plaque enhancement on CTA (31). Further studies are needed to determine whether there is a causal relationship between plaque enhancement, IPH, and PCAT.

Plaque ulceration and soft plaque thickness are also linked to acute ischemic stroke, as reported in previous studies (17,32). However, in our study, we did not find any significant differences in these two factors among the three groups. Sample selection bias could be a possible explanation for the lack of observed differences. Therefore, we need to increase the sample size to further investigate this relationship.

Our study had some limitations. Firstly, our study was a cross-sectional design, which only allows us to establish an association between PCAT attenuation and the period of carotid atherosclerotic disease. A longitudinal study would be necessary to investigate the natural progression of PCAT attenuation following the formation and rupture of carotid plaques. Secondly, our study was limited to a single-center and a small patient cohort, which underwent CTA using a single CT scanner. Future longitudinal studies involving multiple centers and larger sample sizes are required to further investigate the relationship between PCAT attenuation and the risk of acute stroke in patients with carotid atherosclerotic plaque. Moreover, whether patients with carotid atherosclerotic plaque could benefit from this imaging biomarker remains to be investigated using CTA.

Conclusions

PCAT attenuation is a quantitative feature of carotid atherosclerotic inflammation which reliably distinguishes different stages of carotid atherosclerotic disease. This finding suggests that PCAT attenuation could potentially be used to guide preventive and targeted therapies for carotid atherosclerotic disease. However, further confirmation of our results through longitudinal analysis would be necessary to establish the utility of PCAT attenuation in stratifying carotid atherosclerotic disease and tracking patient responses to carotid atherosclerotic disease treatment.

Acknowledgments

The authors thank AiMi Academic Services (www.aimieditor.com) for English language editing and review services.
Funding: This work was supported by the Beijing Hospitals Authority's Ascent Plan (DFL20220303); Beijing Key Specialists in Major Epidemic Prevention and Control.

Footnote

Conflicts of Interest: All authors have completed the ICMJE uniform disclosure form (available at https://qims.amegroups.com/article/view/10.21037/qims-23-454/coif). The authors have no conflicts of interest to declare.

Ethical Statement: The authors are accountable for all aspects of the work in ensuring that questions related to the accuracy or integrity of any part of the work are appropriately investigated and resolved. The study was conducted in accordance with the Declaration of Helsinki (as revised in 2013). The study was approved by the Ethics

Committee of Xuanwu Hospital, and informed consent was obtained from all patients or their legal guardians.

References

1. Barrett KM, Brott TG. Stroke Caused by Extracranial Disease. Circ Res 2017;120:496-501.
2. Cheng SF, Brown MM, Simister RJ, Richards T. Contemporary prevalence of carotid stenosis in patients presenting with ischaemic stroke. Br J Surg 2019;106:872-8.
3. Ross R. Atherosclerosis--an inflammatory disease. N Engl J Med 1999;340:115-26.
4. Mazighi M, Labreuche J, Gongora-Rivera F, Duyckaerts C, Hauw JJ, Amarenco P. Autopsy prevalence of intracranial atherosclerosis in patients with fatal stroke. Stroke 2008;39:1142-7.
5. Labadzhyan A, Csiba L, Narula N, Zhou J, Narula J, Fisher M. Histopathologic evaluation of basilar artery atherosclerosis. J Neurol Sci 2011;307:97-9.
6. Rudd JH, Myers KS, Bansilal S, Machac J, Rafique A, Farkouh M, Fuster V, Fayad ZA. (18)Fluorodeoxyglucose positron emission tomography imaging of atherosclerotic plaque inflammation is highly reproducible: implications for atherosclerosis therapy trials. J Am Coll Cardiol 2007;50:892-6.
7. Rudd JH, Warburton EA, Fryer TD, Jones HA, Clark JC, Antoun N, Johnström P, Davenport AP, Kirkpatrick PJ, Arch BN, Pickard JD, Weissberg PL. Imaging atherosclerotic plaque inflammation with 18F-fluorodeoxyglucose positron emission tomography. Circulation 2002;105:2708-11.
8. Nakajima A, Sugiyama T, Araki M, Seegers LM, Dey D, McNulty I, Lee H, Yonetsu T, Yasui Y, Teng Y, Nagamine T, Nakamura S, Achenbach S, Kakuta T, Jang IK. Plaque Rupture, Compared With Plaque Erosion, Is Associated With a Higher Level of Pancoronary Inflammation. JACC Cardiovasc Imaging 2022;15:828-39.
9. Mancio J, Oikonomou EK, Antoniades C. Perivascular adipose tissue and coronary atherosclerosis. Heart 2018;104:1654-62.
10. Lin A, Nerlekar N, Yuvaraj J, Fernandes K, Jiang C, Nicholls SJ, Dey D, Wong DTL. Pericoronary adipose tissue computed tomography attenuation distinguishes different stages of coronary artery disease: a cross-sectional study. Eur Heart J Cardiovasc Imaging 2021;22:298-306.
11. Pasqualetto MC, Tuttolomondo D, Cutruzzolà A, Niccoli G, Dey D, Greco A, Martini C, Irace C, Rigo F, Gaibazzi N. Human coronary inflammation by computed tomography: Relationship with coronary microvascular dysfunction. Int J Cardiol 2021;336:8-13.
12. Buckler AJ, Karlöf E, Lengquist M, Gasser TC, Maegdefessel L, Perisic Matic L, Hedin U. Virtual Transcriptomics: Noninvasive Phenotyping of Atherosclerosis by Decoding Plaque Biology From Computed Tomography Angiography Imaging. Arterioscler Thromb Vasc Biol 2021;41:1738-50.
13. Sigala F, Oikonomou E, Antonopoulos AS, Galyfos G, Tousoulis D. Coronary versus carotid artery plaques. Similarities and differences regarding biomarkers morphology and prognosis. Curr Opin Pharmacol 2018;39:9-18.
14. Konishi M, Sugiyama S, Sato Y, Oshima S, Sugamura K, Nozaki T, Ohba K, Matsubara J, Sumida H, Nagayoshi Y, Sakamoto K, Utsunomiya D, Awai K, Jinnouchi H, Matsuzawa Y, Yamashita Y, Asada Y, Kimura K, Umemura S, Ogawa H. Pericardial fat inflammation correlates with coronary artery disease. Atherosclerosis 2010;213:649-55.
15. U-King-Im JM, Fox AJ, Aviv RI, Howard P, Yeung R, Moody AR, Symons SP. Characterization of carotid plaque hemorrhage: a CT angiography and MR intraplaque hemorrhage study. Stroke 2010;41:1623-9.
16. Baradaran H, Gupta A. Carotid Vessel Wall Imaging on CTA. AJNR Am J Neuroradiol 2020;41:380-6.
17. Gupta A, Baradaran H, Kamel H, Pandya A, Mangla A, Dunning A, Marshall RS, Sanelli PC. Evaluation of computed tomography angiography plaque thickness measurements in high-grade carotid artery stenosis. Stroke 2014;45:740-5.
18. Saba L, Lanzino G, Lucatelli P, Lavra F, Sanfilippo R, Montisci R, Suri JS, Yuan C. Carotid Plaque CTA Analysis in Symptomatic Subjects with Bilateral Intraparenchymal Hemorrhage: A Preliminary Analysis. AJNR Am J Neuroradiol 2019;40:1538-45.
19. Baradaran H, Myneni PK, Patel P, Askin G, Gialdini G, Al-Dasuqi K, Kamel H, Gupta A. Association Between Carotid Artery Perivascular Fat Density and

Cerebrovascular Ischemic Events. J Am Heart Assoc 2018;7:e010383.
20. Qi XY, Qu SL, Xiong WH, Rom O, Chang L, Jiang ZS. Perivascular adipose tissue (PVAT) in atherosclerosis: a double-edged sword. Cardiovasc Diabetol 2018;17:134.
21. Oikonomou EK, Marwan M, Desai MY, Mancio J, Alashi A, Hutt Centeno E, et al. Non-invasive detection of coronary inflammation using computed tomography and prediction of residual cardiovascular risk (the CRISP CT study): a post-hoc analysis of prospective outcome data. Lancet 2018;392:929-39.
22. Zhang S, Yu X, Gu H, Kang B, Guo N, Wang X. Identification of high-risk carotid plaque by using carotid perivascular fat density on computed tomography angiography. Eur J Radiol 2022;150:110269.
23. Zhang F, Yang L, Gan L, Fan Z, Zhou B, Deng Z, Dey D, Berman DS, Li D, Xie Y. Spotty Calcium on Cervicocerebral Computed Tomography Angiography Associates With Increased Risk of Ischemic Stroke. Stroke 2019;50:859-66.
24. Elkind MS. Inflammatory mechanisms of stroke. Stroke 2010;41:S3-8.
25. Ridker PM, Buring JE, Shih J, Matias M, Hennekens CH. Prospective study of C-reactive protein and the risk of future cardiovascular events among apparently healthy women. Circulation 1998;98:731-3.
26. Ridker PM, Hennekens CH, Buring JE, Rifai N. C-reactive protein and other markers of inflammation in the prediction of cardiovascular disease in women. N Engl J Med 2000;342:836-43.
27. Redgrave JN, Lovett JK, Gallagher PJ, Rothwell PM. Histological assessment of 526 symptomatic carotid plaques in relation to the nature and timing of ischemic symptoms: the Oxford plaque study. Circulation 2006;113:2320-8.
28. Bentzon JF, Otsuka F, Virmani R, Falk E. Mechanisms of plaque formation and rupture. Circ Res 2014;114:1852-66.
29. Hellings WE, Peeters W, Moll FL, Piers SR, van Setten J, Van der Spek PJ, de Vries JP, Seldenrijk KA, De Bruin PC, Vink A, Velema E, de Kleijn DP, Pasterkamp G. Composition of carotid atherosclerotic plaque is associated with cardiovascular outcome: a prognostic study. Circulation 2010;121:1941-50.
30. Millon A, Boussel L, Brevet M, Mathevet JL, Canet-Soulas E, Mory C, Scoazec JY, Douek P. Clinical and histological significance of gadolinium enhancement in carotid atherosclerotic plaque. Stroke 2012;43:3023-8.
31. Saba L, Zucca S, Gupta A, Micheletti G, Suri JS, Balestrieri A, Porcu M, Crivelli P, Lanzino G, Qi Y, Nardi V, Faa G, Montisci R. Perivascular Fat Density and Contrast Plaque Enhancement: Does a Correlation Exist? AJNR Am J Neuroradiol 2020;41:1460-5.
32. Thammongkolchai T, Riaz A, Sundararajan S. Carotid Stenosis: Role of Plaque Morphology in Recurrent Stroke Risk. Stroke 2017;48:e197-9.

Cite this article as: Liu X, Wu F, Jia X, Qiao H, Liu Y, Yang X, Li Y, Zhang M, Yang Q. Pericarotid adipose tissue computed tomography attenuation distinguishes different stages of carotid atherosclerotic disease: a cross-sectional study. Quant Imaging Med Surg 2023;13(12):8247-8258. doi: 10.21037/qims-23-454

